JACS
JOURNAL OF THE AMERICAN CHEMICAL SOCIETY
pubs.acs.org/JACS

Article

G4-Ligand-Conjugated Oligonucleotides Mediate Selective Binding and Stabilization of Individual G4 DNA Structures

Andreas Berner,[‖] Rabindra Nath Das,[‖] Naresh Bhuma,[‖] Justyna Golebiewska, Alva Abrahamsson, Måns Andréasson, Namrata Chaudhari, Mara Doimo, Partha Pratim Bose, Karam Chand, Roger Strömberg, Sjoerd Wanrooij,* and Erik Chorell*

Cite This: *J. Am. Chem. Soc.* 2024, 146, 6926–6935

Read Online

ACCESS | Metrics & More | Article Recommendations | Supporting Information

ABSTRACT: G-quadruplex (G4) DNA structures are prevalent secondary DNA structures implicated in fundamental cellular functions, such as replication and transcription. Furthermore, G4 structures are directly correlated to human diseases such as cancer and have been highlighted as promising therapeutic targets for their ability to regulate disease-causing genes, e.g., oncogenes. Small molecules that bind and stabilize these structures are thus valuable from a therapeutic perspective and helpful in studying the biological functions of the G4 structures. However, there are hundreds of thousands of G4 DNA motifs in the human genome, and a long-standing problem in the field is how to achieve specificity among these different G4 structures. Here, we developed a strategy to selectively target an individual G4 DNA structure. The strategy is based on a ligand that binds and stabilizes G4s without selectivity, conjugated to a guide oligonucleotide, that specifically directs the G4-Ligand-conjugated oligo (GL-O) to the single target G4 structure. By employing various biophysical and biochemical techniques, we show that the developed method enables the targeting of a unique, specific G4 structure without impacting other off-target G4 formations. Considering the vast amount of G4s in the human genome, this represents a promising strategy to study the presence and functions of individual G4s but may also hold potential as a future therapeutic modality.

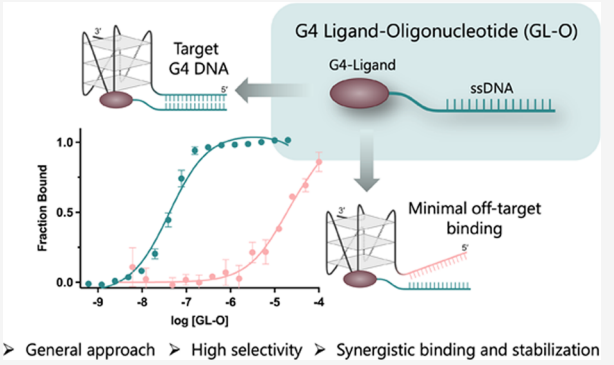

INTRODUCTION

G-quadruplex structures (G4s) are noncanonical four-stranded DNA structures observed in guanine-rich regions of genomes. These structures are composed of square planar arrangements of four guanines (G) that are held together by eight Hoogsteen hydrogen bonds to form G-tetrads. A G4 structure is typically composed of two to four G-tetrads stacked on top of each other and can be highly stable and polymorphic.[1,2] The direction of the G-rich strands and the connecting loops can give the G4 structures different conformations.[2] However, the core of the G4 structures with stacked G-tetrads is always the same.

Computational studies have revealed around 700,000 sequences in the human genome with potential to form G4 structures.[3−6] These sequences showed a nonrandom distribution with G4 motifs located predominantly at e.g., the promoter regions of oncogenes.[4,7] G4 DNA structures are mainly formed in single-stranded G-rich sequences in the course of unwinding of the double helix during different biological processes such as replication, transcription, translation, DNA repair, molecular crowding, and negative supercoiling.[8−10] G4 structures are involved in regulating many cellular processes such as telomeric length maintenance and transcription,[10] but can also be linked to human diseases such as neurodegenerative diseases,[11,12] and different types of cancers.[13,14] For example, the *c-MYC* gene, that is involved in cell cycle regulation and is overexpressed in most cancer types,[15,16] is predominantly regulated by the guanine-rich promoter region (NHEIII) Pu27 which can fold into multiple G4 structures.[17,18]

The ability to silence oncogenes by stabilizing G4 structures in their promoters, like the *c-MYC* G4, has appeared as an attractive novel therapeutic approach and especially for those oncogenes coding for "undruggable" proteins.[13] Indeed, there are vast examples of small organic molecules developed to bind and stabilize G4 DNA with selectivity over double-stranded DNA.[14,19−21] In the cellular context, such ligands have also been observed to downregulate the transcription of oncogenes.[22] In the same way, telomerase activity has been found to

Received: December 19, 2023
Revised: February 19, 2024
Accepted: February 21, 2024
Published: March 2, 2024

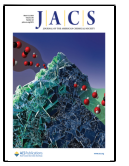

https://doi.org/10.1021/jacs.3c14408
J. Am. Chem. Soc. 2024, 146, 6926−6935

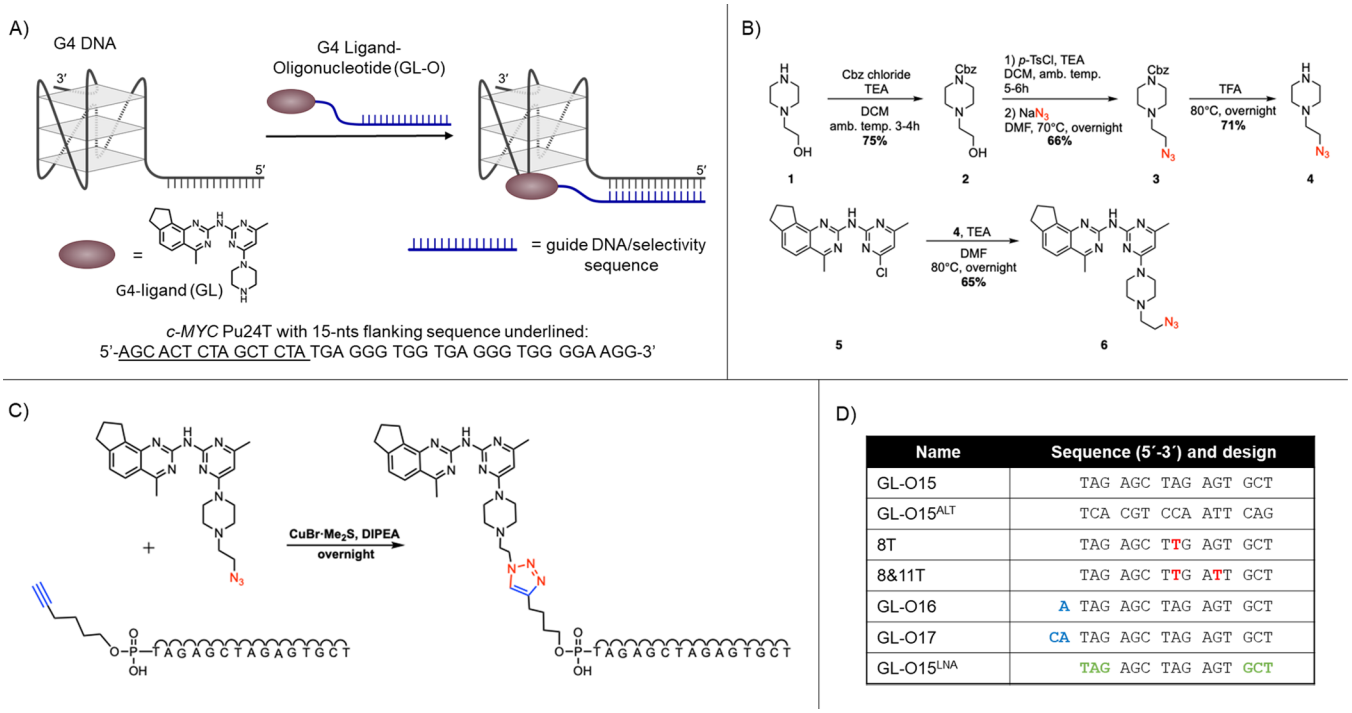

Name	Sequence (5´-3´) and design
GL-O15	TAG AGC TAG AGT GCT
GL-O15^{ALT}	TCA CGT CCA ATT CAG
8T	TAG AGC TTG AGT GCT
8&11T	TAG AGC TTG ATT GCT
GL-O16	A TAG AGC TAG AGT GCT
GL-O17	CA TAG AGC TAG AGT GCT
GL-O15^{LNA}	TAG AGC TAG AGT GCT

Figure 1. Overview of the strategy and chemistry employed in this study. (A) Summary of the presented strategy to target individual G4 DNA structures using G4-ligand-oligonucleotide (GL-O) compounds, G4-ligand correspond to compound number 14a in reference.[28] (B) Synthesis of the azido-functionalized quinazoline-pyrimidine ligand for further conjugations with click chemistry. (C) Conjugation through copper catalyzed click chemistry of the G4-ligand (GL) to the oligonucleotide to give the GL-O15. (D) Overview of some GL-Os used in this study; all compounds are listed in Table S1. Point mutations are indicated in red, extra nucleotides added are indicated in blue and LNA nucleotides are indicated in green.

be inhibited by ligands that can stabilize the telomeric G-quadruplex structures.[23,24] These types of compounds can thus be used to study G4 biology and for further developments toward therapeutics. However, the quantity of G-quadruplex ligands that have proceeded into clinical trials is remarkably low. Compound CX-3543 is one example that entered clinical studies but was eventually withdrawn and its development was discontinued.[13,25] An analogue based on this compound, CX-5461, is now in phase I/II clinical trials for patients with BRCA1/2 deficient tumors.[26,27] The major reason for the slow progression toward clinical trials is likely related to the lack of specificity, as most G4 ligands can bind to several G4 structures, leading to a plethora of side effects considering the hundreds of thousands of G4 motifs in the human genome.

The need for G4 DNA stabilizing compounds able to uniquely recognize only one G4 structure has been highlighted for decades but still with limited-to-no compounds with confirmed specificity. This is mainly ascribed to the fact that the core of G4s is the same between different structures and offers a flat and hydrophobic surface that can be easily targeted with small molecules. However, this binding mode makes it problematic to discriminate among different G4 structures. In this regard, different approaches to gain selectivity have recently started to be explored,[29] such as ligand−peptide conjugates,[30] simultaneous recognition of duplex and quadruplex motifs,[31,32] a DNA molecule that hybridize with the flanking single strand to target RNA G4s,[33] peptide nucleic acid (PNA) derivatives,[34−37] and ligand-PNA conjugates.[38,39] However, the slow progression of selective individual G4 targeting methods highlights the need for diverse approaches.

To meet the need for G4 specific targeting strategies, we use the fact that most G4 ligands bind the terminal G-tetrad of the G4 DNA structure. This enables conjugation of the G4-ligand to an oligonucleotide that base-pairs with the sequence directly flanking the G4 structure. These G4-flanking regions are heterogeneous and differ between each G4, thus allowing specific targeting of individual G4s (Figure 1A). Hence, we have conjugated two recognition motifs; a G4-ligand that targets the terminal G-tetrad of the G4 and a DNA oligonucleotide complementary to the sequence flanking the target G4. The fundamental biochemical process of hybridization between complementary DNA strands into a duplex will guide the G4-ligand-conjugated oligo (GL-O) moiety to the targeted G4 structure. Our hypothesis is that a robust effect, minimizing off-target interactions, is achieved only when both these two recognition motifs can bind simultaneously. We examined this strategy on the Pu24T G4 structure which is a well known model system of the *c-MYC* oncogene Pu27.[40] To challenge the specificity gained by the GL-O approach, different biophysical and biochemical techniques were employed. Taken together, the results show that the developed approach allows for targeting of a distinct, individual G4 structure while leaving other off-target G4s unaffected. We thus developed an approach with potential to modulate gene expression at the DNA level, which in theory could be designed toward any of the hundreds of thousands of potential G4 DNA structures by replacement of the guide oligonucleotide. Compared to previous G4 specific targeting strategies, which largely relies on PNA, the herein presented approach uses guide DNA oligonucleotides to target G4 DNA structures because DNA/RNA has proven the preferred strategy for

https://doi.org/10.1021/jacs.3c14408
J. Am. Chem. Soc. 2024, 146, 6926−6935

oligonucleotide therapeutic applications. Considering the significant developments and successful clinical trials leading to approvals of dozens of oligonucleotide-based therapeutics over the past few years, the proposed strategy may thus hold promise for future therapeutic approaches but also has potential as a valuable tool to explore the cellular function of one specific G4 structure.

RESULTS AND DISCUSSION

Design and Synthesis of G4-Ligand-Conjugated Oligonucleotides (GL-Os). We recently reported on a novel G4-ligand (Figure 1A),[28] that both efficiently binds and stabilizes G4 DNA structures and that has drug-like properties (e.g., no permanent charges and has a low molecular weight), allowing further conjugation to an oligonucleotide guide sequence. To enable conjugation of this G4-Ligand (in this study, renamed GL) to the oligonucleotide sequence, an azido-substituted piperazine side chain was introduced for further conjugation through click chemistry (Figure 1B). The azido-piperazine (**4**) was synthesized starting from the commercially available 2-hydroxyethyl piperazine **1**, which was protected as its benzoylformate (Cbz) derivative **2** by using benzoyl chloroformate (CbzCl). The primary hydroxyl group was next converted into its tosyl derivative, which was subsequently displaced with an azido group using sodium azide to get the piperazine-ethylazido derivative **3** in 66% yield. The Cbz group in **3** was deprotected using TFA at 80 °C, to give the desired piperazine-ethylazido linker **4** in 71% yield. A substitution reaction with this linker (**4**) and chloro-substituted quinazoline-pyrimidine G4-ligand **5** gave the desired azido-functionalized G4-ligand **6** in 65% yield.

After the synthesis of the azido-functionalized G4-ligand, we performed the conjugation step with terminal alkyne modified oligodeoxynucleotide sequences using a copper-mediated click reaction (Figure 1C and Table S2). This enables the production of GL-Os with different guide sequences (Figure 1D and Table S1).

To test the G4-Ligand-conjugated Oligo (GL-O) strategy, we targeted the *c-MYC* Pu24T G4, which is a parallel G4 structure frequently used as model to study the *c-MYC* G4 structure.[40] In our experiments with *c-MYC* Pu24T, we also included a 15-nt oligonucleotide G4-flanking sequence with an AT/GC ratio close to one (1.14) (Figure 1A). This particular 15-nts was selected as the G4-flanking region because circular dichroism (CD) spectroscopy showed that it did not alter the parallel G4 structure topology of *c-MYC* Pu24T. Other G4-flanking sequences were excluded based on CD evaluation since they altered the topology of the *c-MYC* Pu24T G4 structure (Figure S1A). Hereafter, our reference to G4 DNA pertains specifically to the *c-MYC* Pu24T G4 including the flanking sequence that preserves the original topology (Table S1, called R2-Pu24T).

G4-Ligand Maintains G4 Binding Capacity After Guide Oligonucleotide Conjugation. There are today many reported G4 ligands with high affinity, and the main aim of this study is not to improve these but rather to retain the affinity and gain specificity. Therefore, we first investigated if the conjugation of the G4-ligand to a comparatively large oligonucleotide would affect the G4 binding ability by comparing the G4-ligand (GL) alone with the synthesized G4-Ligand-conjugated oligonucleotide (GL-O) in a series of biophysical and in vitro biochemical methods.

With nuclear magnetic resonance (NMR), we can simultaneously study the G4 DNA and duplex DNA formation (annealing of guide oligonucleotide to the 15-nts G4-flanking region). G4 imino signals are found between 10 and 12 PPM while the double-stranded DNA signals appear between 12 and 14 PPM. Thus, the coexistence of double-stranded DNA and G4 DNA can easily be monitored in the same NMR spectrum. We recorded ^{1}H NMR spectra of prefolded G4 DNA alone and in the presence of GL-O15 or O15 (the guide oligonucleotide without G4-ligand) (Figure 2A). The ^{1}H

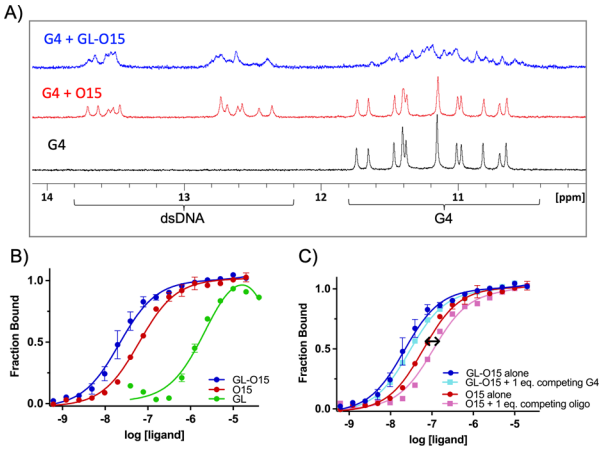

D)

Ligand	Competitor (1 eqiv.)	Binding constant K_d (nM)
GL-O15	-	12 ± 3
O15	-	60 ± 5
GL	-	>200
GL-O15	G4 DNA without flanking sequence	14 ± 2
O15	15-nts oligonucleotide complementary to O15	106 ± 15

Figure 2. Conjugation of the G4-ligand to the guide oligonucleotide retain G4 binding. The recognition sequence guides the ligand without affecting G4 binding. (A) ^{1}H NMR spectra of the G4 DNA (90 μM) (black), in the presence of 1 equiv of O15 (red) and GL-O15 (blue). G4 imino signals appear between 10 and 12 PPM and double-stranded DNA signals appear between 12 and 14 PPM. (B) Dose−response curves obtained from MST analysis of the G4 DNA after the addition of GL-O15, GL-O15, or GL. (C) Dose−response curves obtained from MST analysis of the same G4 DNA as in B after addition of GL-O15 + 1 equiv of *c-MYC* Pu24T G4 DNA without the flanking sequences as competitor or O15 + 1 equiv of 15-nts oligonucleotide complementary to O15 as competitor. (D) K_d values obtained from MST analysis.

NMR spectrum of the G4 DNA with the 15-nts G4-flanking sequence was first recorded, and the G4 imino protons (10.5−11.8 ppm) display a similar pattern to the G4 without the inserted G4-flanking sequence, which again confirmed that the added 15-nts does not substantially affect the fold of the G4 structure (Figure S2A). When one equivalent of O15 is added, new dsDNA signals are observed in the 12.3−13.8 ppm region, indicating hybridization of O15 (Figure 2A). The G4 imino signals are unchanged upon addition of the O15, showing that the pairing of the O15 at the flanking region does not substantially affect the structure or conformation of the *c-MYC* Pu24T G4 structure. Binding of GL to this G4 induce significant changes to the G4 imino signals (10−12 PPM) showing ligand-G4 structure interactions (Figure S2B). GL-O15 binding induces both these changes to the G4 imino signals (10−12 PPM) and the dsDNA signals (12−14 PPM)

https://doi.org/10.1021/jacs.3c14408
J. Am. Chem. Soc. 2024, 146, 6926−6935

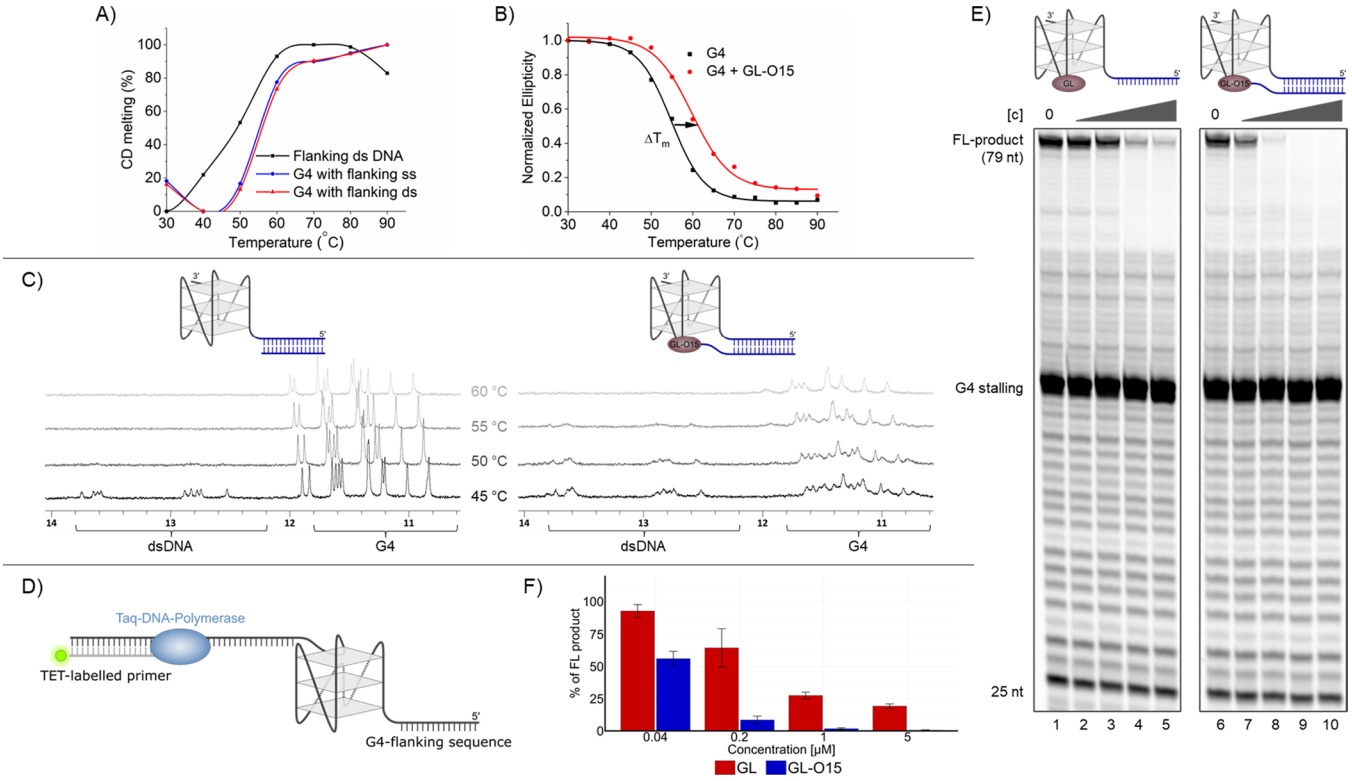

Figure 3. Conjugation of the G4-ligand to the Guide oligonucleotide retain G4 stabilization. Denaturation/melting study of DNA using CD and NMR. (A) CD melting (%) at different wavelengths corresponds to G4 DNA (melting at 263 nm) and dsDNA formed in the presence of O15 (melting at 283 nm). The flanking dsDNA sequence formed in the presence of O15 is melting at a lower temperature compared to the G4 DNA. The presence of a single-stranded or double-stranded flanking sequence does therefore not change the CD melting curve. (B) CD melting curve of G4 DNA in the presence and absence of GL-O15. (C) ^{1}H NMR spectra of the G4 DNA at different temperatures with O15 (left) or GL-O15 (right). Spectra were recorded in 3 mM KCl and 10 mM potassium phosphate buffer (pH = 7.4). For comparison, spectra recorded in 500 μM KCl and 10 mM potassium phosphate buffer (pH = 7.4) are available in Figure S4A,B. (D) Schematic representation of the Polymerase Stop Assay. The TET-labeled primer (gray) is annealed to a G4 forming DNA template (dark gray) and extended by Taq Polymerase (light blue). (E) Taq Polymerase Stop assays in the presence of increasing concentrations (0.04, 0.2, 1, and 5 μM) of GL (lanes 2−5) or GL-O15 (lanes 7−10). (F) Quantification of the Taq polymerase Stop assays in F. The full-length product is expressed in % of the full-length band intensity that was obtained in the control reaction that did not contain the compound. Mean and standard deviation of three individual experiments is shown.

(Figure 2A). The 15-nt flanking sequence thus seem to serve as recognition sequence able to direct the GL-O15 without disturbing the ability of the GL to bind the G4 structure. CD spectroscopy of the G4 DNA confirmed our conclusions from NMR analysis; after addition of GL-O15, we still see the characteristic parallel G4 peaks but also a shoulder at 283−290 nm fitting with dsDNA formation (Figure S3A).

We next used Microscale Thermophoresis (MST) to determine the binding affinity of GL, O15, and GL-O15 to the G4 DNA (Table S1) (Figure 2B−D). The GL has a binding affinity constant, K_d, above 200 nM, whereas the O15 display an affinity of 60 nM (Figure 2B,D). Encouragingly, the GL-O15 compound has a K_d of 12 nM which is considerably stronger than those of both the GL and the O15 alone. This shows that the conjugation of the GL to the oligonucleotide does not negatively affect the binding affinity but on the contrary seems to result in a synergistic binding effect (Figure 2B,D). Furthermore, GL-O15 retains its binding affinity to the G4 with the flanking sequence, even in the presence of one equivalent of competing unlabeled *c-MYC* Pu24T G4 DNA without flanking region (Figure 2C,D). Binding of the O15 oligo alone, however, was outcompeted by addition of one equivalent of an oligonucleotide complementary to O15 (Figure 2C,D).

Conjugation of the G4-Ligand to the Guide Oligonucleotide Retains G4 Stabilization. With the knowledge that GL conjugation to the oligonucleotide did not negatively affect G4 binding but instead resulted in a synergistic improvement, we next investigated whether GL conjugation to the oligonucleotide would also retain its ability to stabilize G4s using DNA melting experiments. CD melting studies with the G4 DNA in the presence of O15 showed a stepwise denaturation with increasing temperatures, where the dsDNA (O15 hybridized to the 15-nts flanking region) is denaturing first followed by the G4 DNA structure (Figures 3A and S3B,C). Addition of GL-O15 results in an increased melting temperature, which shows that the strong binding of GL-O15 to the G4 DNA also translates into stabilization of the G4 DNA structure (Figure 3B). In this assay, the increase in melting temperature was slightly lower compared (Figure S1B) to the experiment with addition of GL alone (without O15). The unbound oligonucleotide of GL-O15 thus prevents the conjugated G4-ligand to stabilize the G4 to its full potential. However, this effect is likely linked to the increased temperature in this assay and the fact that the dsDNA is denaturing at a lower temperature compared to the G4 structure. This could be confirmed by NMR experiments at increased temperatures, which show that the dsDNA peaks (12−14 PPM) disappear around 50 °C and the G4 DNA

https://doi.org/10.1021/jacs.3c14408
J. Am. Chem. Soc. 2024, 146, 6926−6935

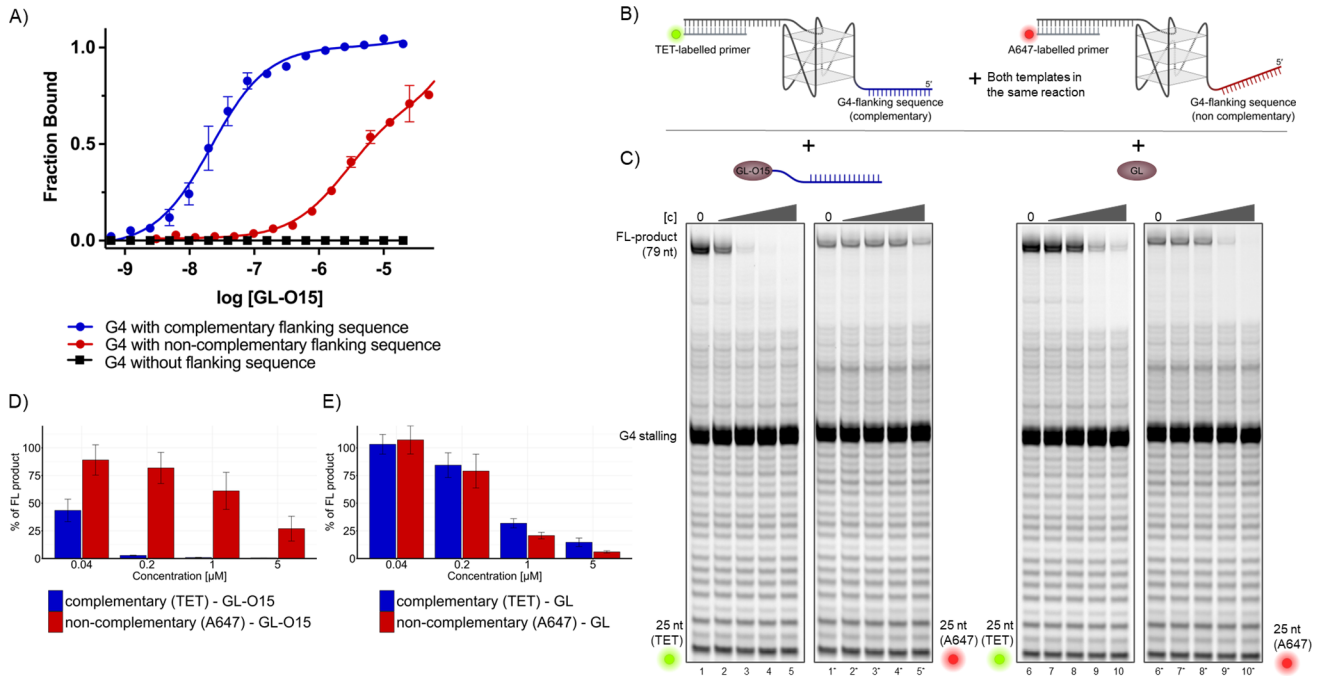

Figure 4. Guide oligonucleotide enhances G4-ligand selectively for an individual G4 structure.(A) Dose−response curves obtained from MST analysis with GL-O15 using *c-MYC* Pu24T G4 DNA with a flanking sequence that is complementary to GL-O15, a noncomplementary flanking sequence, and no flanking sequence. (B) Schematic representation of the Polymerase Stop Assay with two differently labeled templates in the same reaction. Template with a sequence complementary to GL-O15 flanking the G4 was annealed to a 25 nt TET-labeled primer. Template with an alternative flanking sequence (red) was annealed to a 25 nt A647 labeled primer. Both templates were mixed 1:1 and used for Polymerase Stop Assays with (C) GL-O15 (lanes 2−5 and 2′−5′) or GL (lanes 7−10 and 7′−10′) added in increasing concentrations (0.04, 0.2, 1, 5 μM). Left panels of lanes 1−5 and 6−10 represent the scan for the TET label, right panels (lanes marked with ′) represent the scan for A647 of the same lanes. (D) and (E) quantification of the gel shown in (C, D) for GL-O15 (lanes 2−5 and 2′-5′) and (E) for GL (lanes 7−10 and 7′−10′), percentage of full-length (FL) DNA product compared to the control reaction without compound, mean and standard deviation of three individual experiments are shown.

signals (10−12 PPM) are still clearly visible at 65 °C (Figure 3C, left panel, S4C). Interestingly, the dsDNA peaks are still visible (Figure 3C, right panel, S4D) at higher temperatures in the presence of GL-O15 (55 °C) compared to when O15 alone is added (50 °C), showing that binding of GL-O15 to the G4 DNA is also able to stabilize the oligonucleotide hybridization to the 15-nt flanking region.

To further explore how the high affinity of GL-O15 translates into G4 stabilization, we next used a DNA polymerase stop assay. This assay evaluates how efficiently the Taq polymerase can synthesize new DNA by copying a template strand and give a single nucleotide resolution readout by extending a fluorescent 5′ end-labeled DNA primer. A G4 structure is a hurdle for the DNA polymerase, and if a G4 DNA structure is used on the template strand, the Taq polymerase will stall at the G4 structure. However, the DNA polymerase can partly bypass the G4 structure and synthesize to the end of the DNA template producing a full-length (template runoff) DNA product. The proficiency of G4 stabilizing compounds can be determined by their capability to increase DNA polymerase pausing at the G4 structure, consequently reducing the amount of full-length DNA product.

The experiments were carried out on synthetic G4 forming DNA templates that include a 15-nt G4-flanking DNA sequence that was complementary to the guide oligonucleotide sequence of GL-O15 (Figure 3D−F). The DNA substrates were designed such that the DNA polymerase encounters the G4 structure at the 20th base after initiation of DNA synthesis from the 25 nt long TET-labeled primer (Figure 3D, Table S1). The presence of this 3′ overhang template did not affect the overall topology of the G4 structure (Figure S3D).

The DNA polymerase stop assays were performed in the presence of increasing amounts of either GL or GL-O15 and the G4 stabilizing effect was measured by quantification of the full-length product (Figure 3D−F). When GL-O15 is presented with a substrate that contains the complementary sequence, it results in a strong and dose-dependent G4 stabilization, resulting in a strongly reduced formation of full-length product (Figure 3E, lanes 7−10). Notably, in contrast to the insights obtained from thermal CD melting experiments, this new assay reveals that GL-O15 exhibits an enhanced G4 stabilizing ability compared to GL (Figure 3F,E; compare lanes 2−5 with 7−10). This shows that base-pairing of the guide oligonucleotide sequence of GL-O15 to the DNA template in the vicinity of the G4, which primarily serves to guide the ligand to the target, simultaneously enhances its G4 stabilizing capacity.

We next performed DNA polymerase stop assays to investigate if GL-O15 induced reduction of the full-length product (as shown in Figure 3F,E, lanes 7−10 and Figure S4 lanes 16−20) is the additive effect of stalling induced by the oligonucleotide annealing and G4-ligand stabilization. Addition of oligo alone (O15) did reduce the full-length product, a direct consequence of the DNA polymerase running into the annealed oligonucleotide, which generates an oligonucleotide stalling site (Figure S5 lanes 2−5). The reduction of full-length products is substantially stronger when both O15 and GL are added separately to the same reaction (Figure S5, compare

https://doi.org/10.1021/jacs.3c14408
J. Am. Chem. Soc. 2024, 146, 6926−6935

lanes 12−15 with lanes 2−10), most likely due to the additive inhibition of DNA polymerization by (1) the annealed oligonucleotide induced stalling and (2) the G4 stabilization. Interestingly, addition of GL-O15, where the G4-ligand is chemically linked to the guide oligonucleotide, results in an even stronger reduction of full-length DNA product, suggesting a synergistic effect on G4 stabilization (Figure S5, lanes 17−20). Compared to O15 alone, the GL-O15 does not result in any oligonucleotide stalling, suggesting that GL-O15 dissociates from the DNA at the same time as the G4 is resolved by the polymerase. In conclusion, the DNA polymerase stop experiments agree with the biophysical analysis and show that GL conjugation to the oligonucleotide (to form the GL-O15) does not only retain the stabilization effect from the GL but results in a synergistic effect that enhances stabilization of the correct G4 structure.

To evaluate whether our approach is applicable to G4s beyond *c-MYC* G4, we also examined the *c-KIT* and *HelB* G4 structures in primer extension assays (Figure S6). Analogous to our findings with *c-MYC* G4, GL-O15 effectively enhanced G4 stabilization for the *c-KIT* and *HelB* G4s when a complementary flanking region was present on the DNA template. A much stronger reduction of full-length DNA product was observed in the presence of GL-O15 compared to GL for both G4s (*c-KIT*, compare Figure S6 lanes 2−5 with 7−10; *HelB* compare Figure S6 lanes 17−20 with 22−25). This shows that our GL-O strategy in theory can be designed toward any G4 DNA structure by replacement of the guide oligonucleotide.

Guide Oligonucleotide Induces G4-Ligand Selectively for an Individual G4 Structure. To prove that the increased ability of GL-O15 to bind and stabilize the target G4 is specific, we first performed experiments with c-MYC Pu24T that does not contain a complementary flanking region and thus is unable to hybridize with the oligonucleotide (O15) sequence of GL-O15. Encouragingly, we were unable to detect any binding of GL-O15 to c-MYC Pu24T G4 in the absence of a flanking sequence and a strongly reduced binding using a noncomplementary flanking sequence (Figure 4A). To confirm that this selectivity also translates into G4 stabilization, we used the DNA polymerase stop assay with a DNA template containing an alternative (noncomplementary) flanking region. Encouragingly, GL-O15 failed to significantly affect the G4 stability when the G4 had a noncomplementary flanking region (Figure S7A). The G4 stabilization effect was regained by altering GL-O15's guide sequence to match the sequence flanking the G4, GL-O15^{ALT} (Figure S7A−C). Thus, GL-O15 stabilizes only the G4 with a flanking sequence that is complementary to its guide sequence, which is further supported by binding affinity data (Figure S7B,C).

Importantly, GL-O15 is less proficient in stabilizing G4 structures compared to GL when the complementary DNA template sequence is absent (Figure S7A compare lanes 12−15 with lanes 7−10 and 17−20). Combined with the strong binding affinity and G4 stabilization observed from GL-O15 with the correct complementary flanking region (Figures 2D, 3F, and S7), this suggests that the guide oligonucleotide sequence of GL-O15 hinders the interaction with the G4 structure in the absence of a complementary sequence on the DNA template, which is of central importance to avoid off-target effects of the approach.

To challenge the specificity, we next performed DNA polymerase stop assays with two competitive G4-containing DNA templates in the same reaction tube, one having a flanking sequence complementary to O15 and another DNA template with an alternative noncomplementary flanking sequence (Figure 4B). To distinguish between the DNA products, the noncomplementary flanking sequence (which does not form duplex DNA with GL-O15) is A647 labeled, while the DNA substrate with a flanking region complementary to GL-O15 is TET-labeled. The control compound (GL) did not discriminate between the two sequences and showed a similar ability to stabilize the G4 structure on both DNA templates (Figure 4C,E). In the presence of 1 μM GL, a reduction of about 75% of the full-length product was detected from both DNA substrates (Figure 4C, lanes 9 and 9′). On the contrary, GL-O15 addition displayed an impressive selectivity to the TET-labeled DNA template that carries the complementary flanking sequence. A strong reduction (over 90% at 0.2 μM and about 50% at 0.04 μM GL-O15) of full-length product was detected with TET, indicating strong stabilization of the G4 when the complementary flanking region is present (Figure 4C, lanes 2−5, and 4D). The G4 stabilization effect with the noncomplementary flanking sequence, however, was really weak as indicated by the modest reduction of the A647 signal (around 100−1000 times more GL-O15 was needed for the same effect) (Figure 4C, lanes 2′−5′, and 4D).

Our experiments have now demonstrated that the GL-O approach results in a synergistic effect that selectively increases the stabilization effect of the target G4 (G4s with a flanking complementary DNA sequence, Figures 3 and S4). Furthermore, the approach actively decreases the unspecific G4 stabilization (nontarget G4s with a noncomplementary flanking DNA sequence, Figures 4 and S7). The oligonucleotide conjugation thus specifically guides the GL to the target G4 structure, increases the binding and stabilization of this G4 structure, and prevent off-target interactions.

Nucleotide Gap Size Between the G4 Structure and Duplex DNA Formation Exhibits a Degree of Flexibility. The space between the G4 structure and the base-pairing location of the oligonucleotide sequence from GL-O could be critical for its binding and stabilization capacity. To experimentally address this parameter, we synthesized two compounds, GL-O16 and GL-O17, in which we increased the length of the guide oligonucleotide fragment compared to GL-O15. The guide oligonucleotide sequence of these molecules was designed to base-pair with the complementary flanking region, 3-nts (GL-O15), 2-nts (GL-O16), or 1-nt (GL-O17) away from the G4 structure (Figure S8A). MST analysis showed that the GL-O16 and GL-O17 derivatives displayed similar binding affinities compared to GL-O15, suggesting that these nucleotide gap alterations tested are not crucial for GL-O binding (Figure S8B−D).

To determine the effect of the nucleotide gap size on G4 stabilization, we performed DNA polymerase stop assays on a *c-MYC* Pu24T containing DNA template that allows hybridization of the oligo fragment of the GL-O15, GL-O16, and GL-O17 compounds. The compounds demonstrated no substantial variation in their capacity to stabilize the G4 structure; when utilizing 0.04 μM of each compound, the reduction of full-length DNA products was consistently around 50% in all instances (Figure S8E,F). This suggests that the GL-O design is not strictly limited to the initially tested 3-nt gap size (between the G4 structure and GL-O hybridization), but there is instead a degree of design flexibility for GL-Os in selecting the guide oligonucleotide sequence based on the G4-flanking region.

https://doi.org/10.1021/jacs.3c14408
J. Am. Chem. Soc. 2024, 146, 6926−6935

GL-O Compounds can Differentiate Between G4s with Highly Similar Flanking Regions. We have shown that our GL-O approach does not substantially affect G4s in the absence of any complementary flanking region or with a noncomplementary flanking sequence. However, within the human genome, there are hundreds of thousands of potential G4 DNA structures. Given this vast number, it is likely that some G4 structures will display sequence homology to the target sequence, potentially influencing the selectivity of our GL-O approach. To investigate this possibility, we altered the nucleotides at specific positions of the guide oligonucleotides. All single nucleotide alterations tested did not alter the G4 stabilization ability of the GL-O (Figure 5B, lanes 2−5 and Figure S9 lanes 7−10, 12−15, 22−25, and 27−30).

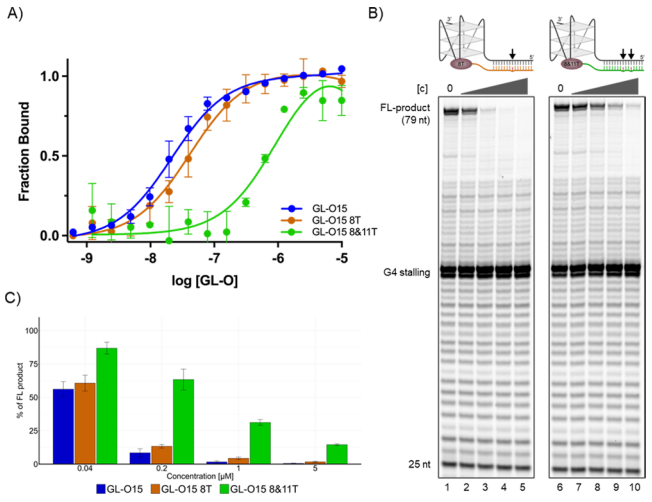

Figure 5. G4 stabilization capability of the GL-O is affected by mismatches in the middle of the oligo.(A) Dose−response curve obtained from MST analysis after addition of GL-O15, GL-O15 8T and GL-O15 8&11T to *c-MYC* Pu24T G4 DNA with the complementary sequence to GL-O15. Error bars correspond to SD of two independent measurements. (B) Polymerase Stop Assays in the presence of increasing concentrations (0.04, 0.2, 1, and 5 μM) of GL-O15 8T (lanes 2−5) or with GL-O15 8&11T (lane 7−10). (C) Quantification of B, percentage of full-length product compared to the control reaction without compound, and mean and standard deviation of three individual experiments are shown.

Similarly, 2-nucleotide alterations at both ends of the guide oligonucleotide did not considerably affect selectivity (Figure S9 lanes 17−20 and 32−35). In contrast, 2 mismatches in the center of the guide oligonucleotide greatly influenced the ability of the GL-O (GL-O15 8 and 11T) to both stabilize and bind the G4 structure (Figure 5). This demonstrates that the GL-O compounds can discriminate against off-target flanking regions that display great sequence similarity.

Locked Nucleic Acids (LNA) is Required to Efficiently Compete with Flanking dsDNA Sequences. G4 DNA predominantly forms in single-stranded DNA, and the details of how double-stranded DNA (dsDNA) reforms in proximity to the G4 structure (the flanking region) are not entirely clear. For the *c-MYC* Pu27 G4, previous studies have shown a stretch of ssDNA (14 nts in length) flanking the 5′ region of the G4.[41] However, the existence and length of ssDNA stretches associated with G4 structures are likely to vary among different G4s in the genome. This variability could significantly influence the efficiency of the GL-O approach. Notably, shorter ssDNA stretches flanking G4s may have a negative impact due to the necessity for strand invasion by the GL-O.

To investigate this aspect, we preannealed a 20-nt complementary DNA oligo to the G4-containing DNA substrate (Figure 6A), effectively reconstructing a G4 structure

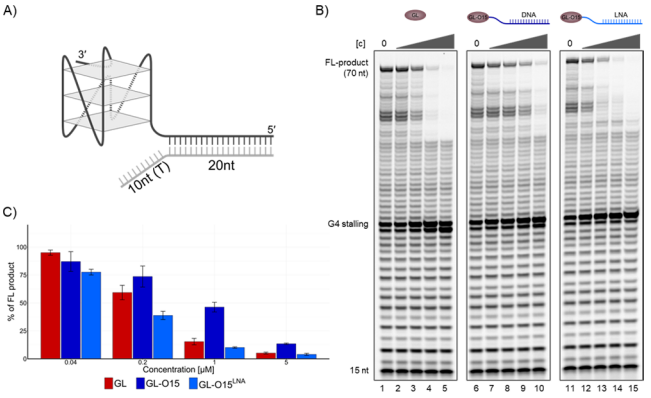

Figure 6. Addition of LNA to the oligo allows invasion of dsDNA for G4 stabilization.(A) Schematic of the substrate design. A G4-containing oligo with 20-nt flanking sequence at the 5′-end was annealed to a 30-nt oligonucleotide, comprising 20 nts complementary to the substrate, and an additional 10-nt T10 overhang, representing the ssDNA typically located opposite the G4 structure. (B) Polymerase Stop Assays in the presence of increasing concentrations (0.04, 0.2, 1, and 5 μM) of GL (lanes 2−5), GL-O15 (lane 7−10), or GL-O15^{LNA} (lanes 12−15). (C) Quantification of B, percentage of full-length product compared to the control reaction without compound, mean and standard deviation of three individual experiments are shown.

with an adjacent dsDNA flanking region. To simulate the ssDNA typically opposite a G4 structure in vivo (a C-rich region), we utilized a T10 overhang (Figure 6A). When this setup was applied in the DNA polymerase stop assay, it reduced the ability of the GL-O to stabilize the G4 (Figure 6B), which can be attributed to the GL-O's inability to form dsDNA on this specific DNA substrate. This made the GL-O less potent as a G4 stabilizer compared to GL alone (Figure 6B, compare lanes 2−5 with lanes 7−10). Consequently, this suggests that the GL-O method may be restricted to G4 structures with characteristics similar to c-MYC Pu27, particularly those that possess a single-stranded DNA segment adjacent to the 5′ region.

To overcome this limitation, we replaced three nucleotides at both the 3′ and 5′ ends of the oligonucleotide in the GL-O with LNA, aiming to improve binding affinity. Indeed, this modification (GL-O15^{LNA}) increased the binding affinity and G4 stabilization, as measured by MST and DNA polymerase stop assays (Figure S10). Importantly, GL-O15^{LNA} also substantially enhanced G4 stabilization when the direct G4-flanking region consisted of dsDNA (Figure 6B,C). This effect was dependent on the conjugation of the GL to the O15^{LNA} to generate the GL-O15^{LNA} because the addition of O15^{LNA} alone showed a comparable G4 stalling to O15^{DNA} alone (Figure S10D,E). This advancement highlights the adaptability of the GL-O approach and the potential for further refinement, tailoring it to the unique requirements of the specific target G4.

CONCLUSIONS

In this work, we developed a strategy based on an unspecific G4-ligand that is conjugated to a DNA oligonucleotide that

https://doi.org/10.1021/jacs.3c14408
J. Am. Chem. Soc. 2024, 146, 6926−6935

guides the ligand to only the target G4 structure, leading to selective binding and stabilization of a specific G4 structure. The approach thus combines two recognition devices, one that identifies the correct position in the genome and the other that selectively binds and stabilizes G4 DNA. We show that conjugation of the G4-ligand to the guide DNA oligonucleotide does not negatively affect the ability to bind and stabilize G4s. Instead, when conjugated, the G4-ligand and the guide DNA oligonucleotide work in synergy to give higher binding affinities and stabilization than when acting as individual components (Figures 2, 3, and S5). The effect is diminished if only one of them can bind, and off-target effects should therefore be largely be avoided. Importantly, we show that the GL-O approach is highly specific to only the target G4 structure and can discriminate between off-target flanking regions with great sequence similarity (Figures 4, 5, and S7).

Furthermore, the distance between the guide sequence and the G4-ligand is open for some level of freedom, which can prove to be highly useful in the design of GL-Os to novel targets (Figure S8). Finally, we introduced LNA in the oligonucleotide backbone of the GL-O, which improved binding affinity and G4 stabilization and enabled strand invasion of dsDNA sequences flanking G4s (Figures 6 and S10). This highlights an important strength of the GL-O strategy as the developments in oligonucleotide modifications now allows great possibilities to tune key properties and affinity. Previous methods aiming at G4 specificity that share some resemblance to the herein presented GL-O approach are generally based on PNA.[29,38] While PNA presents certain advantages such as chemical resistance, the hurdles in, e.g., solubility, delivery, clearance, and immunogenicity linked to PNA has elevated DNA/RNA as the method of choice for therapeutic applications. However, recognizing the infancy of individual G4 targeting, we advocate for an open exploration of all promising methodologies.

In summary, our presented strategy offers a highly modular approach to specifically target individual G4 structures, which in theory could be used to target any of the hundreds of thousands of potential G4 DNA structures. When considering the diverse regulatory roles of G4s, the presented approach opens up detailed future studies of G4 biology and potential therapeutic interventions. In the following studies, we will test our GL-O targeting strategy for individual G4s within a cellular environment.

MATERIALS AND METHODS

G4-Ligand Conjugation of Oligonucleotides through Click Chemistry. A 50 μL aliquot of 1 mM oligonucleotide stock was transferred to an Eppendorf tube to which reagents were added in the following order: G4-ligand (compound 6) (5 equiv of 10 mM stock in DMSO/ACN, 3:7), aqueous DIPEA solution (2.5 μL, 0.25 μmol (5 equiv), 0.043 μL), and CuBr·Me_2S solution in DMSO (7.5 μL, 0.5 μmol (10 equiv), 0.1 mg). The reaction mixture was vortexed and subsequently agitated at ambient temperature overnight. The reaction mixture was diluted with 25 μL of 0.5 mM EDTA solution and 200 μL of water before purification by RP-HPLC. RP-HPLC was done using a C18 semipreparative column with 3 mL/min flow rate and a linear gradient of 5−60% buffer B (100% ACN). Buffer A was 50 mM triethylammonium acetate. The conjugated product was confirmed with HRMS.

Microscale Thermophoresis. G4 DNA labeled with Cy5 at the 5′ end was folded in 10 mM potassium phosphate and 100 mM KCl (pH 7.4) by heating at 95 °C for 5 min, followed by cooling down to room temperature. All MST experiments were performed in 10 mM potassium phosphate (pH 7.4), 100 mM KCl, 0.05% Tween 20, and the labeled G4 DNA concentration was held constant at 20 nM. For titration of GL, concentration varied from 0.6 nM to 2.5 μM (13 dilution steps). For oligos or ligand-conjugated oligos, the maximum concentration was fixed at 20 nM and subsequently 1/2 diluted for 16 steps. The samples were loaded into standard MST grade glass capillaries, and the MST experiment was performed using a Monolith NT.115 (Nano Temper, Germany). For the competition assays, 1 equiv of prefolded Pu24T G4 DNA without flanking sequences or 15-nts were mixed with the Cy5 labeled *c-MYC* Pu24T G4 structure with flanking sequence and MST traces were recorded in the presence of different concentrations of oligos or ligand-conjugated oligos. MST traces were plotted using OriginPro 8.5, and K_d values were generated by the NanoTemper analysis software. Graphs were further plotted in GraphPad Prism 9.0 for visualization.

NMR. The G4 DNA stock solution was prepared by folding 100 μM G4 sequences in 10 mM potassium phosphate buffer (pH = 7.4) and 3000 or 500 μM KCl by heating to 95 °C and slowly cooling down to room temperature. 90 μM of effective DNA concentration was obtained by adding 10% D_2O to the folded G4 DNA solution. 90 μM of O15/GL-O15 was added to the G4 DNA solution, and formation of double standard DNA was monitored. The samples were loaded in 3 mm NMR tubes, and ^{1}H NMR spectra were recorded at 298 K on a Bruker 850 MHz Avance III HD spectrometer equipped with a 5 mm TCI cryoprobe. Transmitter frequency offset (O1P) was set at 4.7 PPM and spectral width (SW) was fixed as 22 ppm. Excitation sculpting was used in the 1D ^{1}H experiments, and 256 scans were used to record the spectra. For variable temperature NMR, ^{1}H NMR spectra were recorded at 5 °C interval and up to 60 °C/70 °C. The temperature of the probe was increased manually, and it was allowed to be stable for five min before recording the spectra. Processing of the spectra were performed in Topspin 4.1.4 (Bruker Biospin, Germany).

Circular Dichroism. Three μM amount of G4 DNA was folded in 10 mM K-phosphate buffer (pH 7.4), with 3 mM KCl by heating for 5 min at 95 °C and then allowed to cool to room temperature. A quartz cuvette with a path length of 1 mm was used for the measurements by a JASCO-720 spectropolarimeter (Jasco international Co. Ltd.). CD spectra were recorded at 25 °C and λ = 210−350 nm with an interval of 0.2 nm and a scan rate of 100 nm/min. Thermal melting curves for G4 DNA were recorded at 263 nm between 20 and 95 °C at a speed of 1 °C/min. Melting temperature (T_m) is defined as the temperature at which 50% of the G4 structures are unfolded.

Taq Polymerase Stop Assay. The Taq Polymerase Stop assay was adapted from Jamroskovic et al.[19] DNA templates were annealed to fluorescent-labeled primers in 100 mM KCl by heating to 95 °C for 5 min followed by slow cooling to room temperature (Table S1). For strand invasion experiments (Figure 6), primer (15-nt-TET) and complementary oligo O20-T(10) were annealed to the template at the same time. The indicated compound concentrations were added to 40 nM annealed template (40 nM of each substrate in the competition assay, Figure 4) in 1× Taq buffer (10 mM Tris-HCl pH 8.8, 50 mM KCl, Thermo Fisher Scientific), 1.5 mM $MgCl_2$, and 0.05 U/μL Taq polymerase (Thermo Fisher Scientific). Samples were preincubated on ice (10 min) and reactions initiated with the addition of dNTPS (100 μM) and transferring the samples to 37 °C. After 15 min at 37 °C reactions were stopped by addition of equal volume of 2× stop solution (0.5% SDS, 25 mM EDTA, XC-Dye in Formamide) and separated on a 12% polyacrylamide Tris-borate-EDTA (TBE) gel containing 25% formamide and 8 M urea. Fluorescent signal was detected with a Typhoon Scanner (Amersham Biosciences). The intensity of the full-length band was quantified using Image Quant TL 10.2 software (GE Healthcare Life Sciences) and compared to the sample without compound.

ASSOCIATED CONTENT

Supporting Information

The Supporting Information is available free of charge at https://pubs.acs.org/doi/10.1021/jacs.3c14408.

https://doi.org/10.1021/jacs.3c14408
J. Am. Chem. Soc. 2024, 146, 6926−6935

Oligonucleotides used in this study; additional CD and NMR experiments; MST and Polymerase Stop Assay control experiments; general experimental details; and NMR Spectra of Synthesised Compounds (PDF)

AUTHOR INFORMATION

Corresponding Authors

Sjoerd Wanrooij − *Department of Medical Biochemistry and Biophysics, Umeå University, Umeå 901 87, Sweden;* orcid.org/0000-0001-6126-4382; Email: sjoerd.wanrooij@umu.se

Erik Chorell − *Department of Chemistry, Umeå University, Umeå 901 87, Sweden;* orcid.org/0000-0003-2523-1940; Email: erik.chorell@umu.se

Authors

Andreas Berner − *Department of Medical Biochemistry and Biophysics, Umeå University, Umeå 901 87, Sweden;* orcid.org/0000-0001-7864-8403

Rabindra Nath Das − *Department of Chemistry, Umeå University, Umeå 901 87, Sweden;* orcid.org/0000-0001-6347-2169

Naresh Bhuma − *Department of Chemistry, Umeå University, Umeå 901 87, Sweden*

Justyna Golebiewska − *Department of Chemistry, Umeå University, Umeå 901 87, Sweden*

Alva Abrahamsson − *Department of Chemistry, Umeå University, Umeå 901 87, Sweden;* orcid.org/0009-0004-3292-1637

Måns Andréasson − *Department of Chemistry, Umeå University, Umeå 901 87, Sweden*

Namrata Chaudhari − *Department of Medical Biochemistry and Biophysics, Umeå University, Umeå 901 87, Sweden*

Mara Doimo − *Department of Medical Biochemistry and Biophysics, Umeå University, Umeå 901 87, Sweden*

Partha Pratim Bose − *Department of Biosciences and Nutrition, Karolinska Institutet, Neo, Huddinge 141 57, Sweden;* orcid.org/0000-0003-4387-3584

Karam Chand − *Department of Chemistry, Umeå University, Umeå 901 87, Sweden;* orcid.org/0000-0001-7691-4392

Roger Strömberg − *Department of Biosciences and Nutrition, Karolinska Institutet, Neo, Huddinge 141 57, Sweden;* orcid.org/0000-0002-7902-2688

Complete contact information is available at: https://pubs.acs.org/10.1021/jacs.3c14408

Author Contributions

‖A.B., R.N.D., and N.B. are equally contributing first authors. * E.C. and S.W. are equally contributing corresponding authors.

Funding

Work in the Chorell lab was supported by the Kempe Foundations (JCK-3159 and SMK-1632), the Swedish Research Council (VR-NT 2017-05235 and VR-NT 2021-04805), and the Cancer Research Foundation in Northern Sweden (AMP 19-968). Work in the Wanrooij lab was supported by the Knut and Alice Wallenberg Foundation, Kempe Foundations (SMK21-0059), and the Swedish Research Council (VR-MH 2018-0278).

Notes

The authors declare no competing financial interest.

REFERENCES

(1) Lane, A. N.; Chaires, J. B.; Gray, R. D.; Trent, J. O. Stability and kinetics of G-quadruplex structures. *Nucleic Acids Res.* **2008**, *36*, 5482−5515.

(2) Burge, S.; Parkinson, G. N.; Hazel, P.; Todd, A. K.; Neidle, S. Quadruplex DNA: sequence, topology and structure. *Nucleic Acids Res.* **2006**, *34*, 5402−5415.

(3) Bedrat, A.; Lacroix, L.; Mergny, J. L. Re-evaluation of G-quadruplex propensity with G4Hunter. *Nucleic Acids Res.* **2016**, *44*, 1746−1759.

(4) Chambers, V. S.; Marsico, G.; Boutell, J. M.; Di Antonio, M.; Smith, G. P.; Balasubramanian, S. High-throughput sequencing of DNA G-quadruplex structures in the human genome. *Nat. Biotechnol.* **2015**, *33*, 877−881.

(5) Hänsel-Hertsch, R.; Beraldi, D.; Lensing, S. V.; Marsico, G.; Zyner, K.; Parry, A.; Di Antonio, M.; Pike, J.; Kimura, H.; Narita, M.; et al. G-quadruplex structures mark human regulatory chromatin. *Nat. Genet.* **2016**, *48*, 1267−1272.

(6) Huppert, J. L.; Balasubramanian, S. Prevalence of quadruplexes in the human genome. *Nucleic Acids Res.* **2005**, *33*, 2908−2916.

(7) Huppert, J. L.; Balasubramanian, S. G-quadruplexes in promoters throughout the human genome. *Nucleic Acids Res.* **2007**, *35*, 406−413.

(8) Eddy, J.; Maizels, N. Gene function correlates with potential for G4 DNA formation in the human genome. *Nucleic Acids Res.* **2006**, *34*, 3887−3896.

(9) Kanoh, Y.; Matsumoto, S.; Fukatsu, R.; Kakusho, N.; Kono, N.; Renard-Guillet, C.; Masuda, K.; Iida, K.; Nagasawa, K.; Shirahige, K.; et al. Rif1 binds to G quadruplexes and suppresses replication over long distances. *Nat. Struct. Mol. Biol.* **2015**, *22*, 889−897.

(10) Rhodes, D.; Lipps, H. J. G-quadruplexes and their regulatory roles in biology. *Nucleic Acids Res.* **2015**, *43*, 8627−8637.

(11) Simone, R.; Fratta, P.; Neidle, S.; Parkinson, G. N.; Isaacs, A. M. G-quadruplexes: Emerging roles in neurodegenerative diseases and the non-coding transcriptome. *FEBS Lett.* **2015**, *589*, 1653−1668.

(12) Wang, E.; Thombre, R.; Shah, Y.; Latanich, R.; Wang, J. G-Quadruplexes as pathogenic drivers in neurodegenerative disorders. *Nucleic Acids Res.* **2021**, *49*, 4816−4830.

(13) Balasubramanian, S.; Hurley, L. H.; Neidle, S. Targeting G-quadruplexes in gene promoters: a novel anticancer strategy? *Nat. Rev. Drug Discovery* **2011**, *10*, 261−275.

(14) Kosiol, N.; Juranek, S.; Brossart, P.; Heine, A.; Paeschke, K. G-quadruplexes: a promising target for cancer therapy. *Mol. Cancer* **2021**, *20*, 40.

(15) Ambrus, A.; Chen, D.; Dai, J.; Jones, R. A.; Yang, D. Solution structure of the biologically relevant G-quadruplex element in the human c-MYC promoter Implications for G-quadruplex stabilization. *Biochemistry* **2005**, *44*, 2048−2058.

(16) Dang, C. V. MYC on the path to cancer. *Cell* **2012**, *149*, 22−35.

(17) Simonsson, T.; Pecinka, P.; Kubista, M. DNA tetraplex formation in the control region of c-myc. *Nucleic Acids Res.* **1998**, *26*, 1167−1172.

(18) Seenisamy, J.; Rezler, E. M.; Powell, T. J.; Tye, D.; Gokhale, V.; Joshi, C. S.; Siddiqui-Jain, A.; Hurley, L. H. The Dynamic Character of the G-Quadruplex Element in the c-MYC Promoter and Modification by TMPyP4. *J. Am. Chem. Soc.* **2004**, *126*, 8702−8709.

(19) Jamroskovic, J.; Doimo, M.; Chand, K.; Obi, I.; Kumar, R.; Brännström, K.; Hedenstrom, M.; Das, R. N.; Akhunzianov, A.; Deiana, M.; et al. Quinazoline Ligands Induce Cancer Cell Death through Selective STAT3 Inhibition and G-Quadruplex Stabilization. *J. Am. Chem. Soc.* **2020**, *142*, 2876−2888.

(20) Jamroskovic, J.; Livendahl, M.; Eriksson, J.; Chorell, E.; Sabouri, N. Identification of Compounds that Selectively Stabilize Specific G-Quadruplex Structures by Using a Thioflavin T-Displacement Assay as a Tool. *Chem.—Eur. J.* **2016**, *22*, 18932−18943.

(21) Prasad, B.; Doimo, M.; Andreasson, M.; L'Hote, V.; Chorell, E.; Wanrooij, S. A complementary chemical probe approach towards customized studies of G-quadruplex DNA structures in live cells. *Chem. Sci.* **2022**, *13*, 2347−2354.

(22) Carvalho, J.; Mergny, J. L.; Salgado, G. F.; Queiroz, J. A.; Cruz, C. G-quadruplex, Friend or Foe: The Role of the G-quartet in Anticancer Strategies. *Trends Mol. Med.* **2020**, *26*, 848−861.
(23) Sun, D.; Thompson, B.; Cathers, B. E.; Salazar, M.; Kerwin, S. M.; Trent, J. O.; Jenkins, T. C.; Neidle, S.; Hurley, L. H. Inhibition of Human Telomerase by a G-Quadruplex-Interactive Compound. *J. Med. Chem.* **1997**, *40*, 2113−2116.
(24) Wheelhouse, R. T.; Sun, D.; Han, H.; Han, F. X.; Hurley, L. H. Cationic Porphyrins as Telomerase Inhibitors: the Interaction of Tetra-(N-methyl-4-pyridyl)porphine with Quadruplex DNA. *J. Am. Chem. Soc.* **1998**, *120*, 3261−3262.
(25) Drygin, D.; Siddiqui-Jain, A.; O'Brien, S.; Schwaebe, M.; Lin, A.; Bliesath, J.; Ho, C. B.; Proffitt, C.; Trent, K.; Whitten, J. P.; et al. Anticancer Activity of CX-3543: A Direct Inhibitor of rRNA Biogenesis. *Cancer Res.* **2009**, *69*, 7653−7661.
(26) Xu, H.; Di Antonio, M.; McKinney, S.; Mathew, V.; Ho, B.; O'Neil, N. J.; Dos Santos, N.; Silvester, J.; Wei, V.; Garcia, J.; et al. CX-5461 is a DNA G-quadruplex stabilizer with selective lethality in BRCA1/2 deficient tumours. *Nat. Commun.* **2017**, *8*, 14432.
(27) Hilton, J.; Gelmon, K.; Bedard, P. L.; Tu, D. S.; Xu, H.; Tinker, A. V.; Goodwin, R.; Laurie, S. A.; Jonker, D.; Hansen, A. R.; et al. Results of the phase I CCTG IND.231 trial of CX-5461 in patients with advanced solid tumors enriched for DNA-repair deficiencies. *Nat. Commun.* **2022**, *13*, 3607.
(28) Bhuma, N.; Chand, K.; Andréasson, M.; Mason, J.; Das, R. N.; Patel, A. K.; Öhlund, D.; Chorell, E. The effect of side chain variations on quinazoline-pyrimidine G-quadruplex DNA ligands. *Eur. J. Med. Chem.* **2023**, *248*, No. 115103.
(29) Cadoni, E.; De Paepe, L.; Manicardi, A.; Madder, A. Beyond small molecules: targeting G-quadruplex structures with oligonucleotides and their analogues. *Nucleic Acids Res.* **2021**, *49*, 6638−6659.
(30) Redman, J. E.; Granadino-Roldan, J. M.; Schouten, J. A.; Ladame, S.; Reszka, A. P.; Neidle, S.; Balasubramanian, S. Recognition and discrimination of DNA quadruplexes by acridine-peptide conjugates. *Org. Biomol. Chem.* **2009**, *7*, 76−84.
(31) Nguyen, T. Q. N.; Lim, K. W.; Phan, A. T. A Dual-Specific Targeting Approach Based on the Simultaneous Recognition of Duplex and Quadruplex Motifs. *Sci. Rep.* **2017**, *7*, 11969.
(32) Asamitsu, S.; Obata, S.; Phan, A. T.; Hashiya, K.; Bando, T.; Sugiyama, H. Simultaneous Binding of Hybrid Molecules Constructed with Dual DNA-Binding Components to a G-Quadruplex and Its Proximal Duplex. *Chem.—Eur. J.* **2018**, *24*, 4428−4435.
(33) Chen, S. B.; Hu, M. H.; Liu, G. C.; Wang, J.; Ou, T. M.; Gu, L. Q.; Huang, Z. S.; Tan, J. H. Visualization of NRAS RNA G-Quadruplex Structures in Cells with an Engineered Fluorogenic Hybridization Probe. *J. Am. Chem. Soc.* **2016**, *138*, 10382−10385.
(34) Gorai, A.; Chaudhuri, R.; Mukhopadhyay, T. K.; Datta, A.; Dash, J. Thiazole Containing PNA Mimic Regulates c-MYC Gene Expression through DNA G-Quadruplex. *Bioconjugate Chem.* **2022**, *33*, 1145−1155.
(35) Sarkar, S.; Armitage, B. A. Targeting a Potential G-Quadruplex Forming Sequence Found in the West Nile Virus Genome by Complementary Gamma-Peptide Nucleic Acid Oligomers. *ACS Infect. Dis.* **2021**, *7*, 1445−1456.
(36) Cadoni, E.; De Paepe, L.; Colpaert, G.; Tack, R.; Waegeman, D.; Manicardi, A.; Madder, A. A red light-triggered chemical tool for sequence-specific alkylation of G-quadruplex and I-motif DNA. *Nucleic Acids Res.* **2023**, *51*, 4112−4125.
(37) Tan, D. J. Y.; Das, P.; Winnerdy, F. R.; Lim, K. W.; Phan, A. T. Guanine anchoring: a strategy for specific targeting of a G-quadruplex using short PNA LNA and DNA molecules. *Chem. Commun.* **2020**, *56*, 5897−5900.
(38) Tassinari, M.; Zuffo, M.; Nadai, M.; Pirota, V.; Sevilla Montalvo, A. C.; Doria, F.; Freccero, M.; Richter, S. N. Selective targeting of mutually exclusive DNA G-quadruplexes: HIV-1 LTR as paradigmatic model. *Nucleic Acids Res.* **2020**, *48*, 4627−4642.
(39) Paul, A.; Sengupta, P.; Krishnan, Y.; Ladame, S. Combining G-Quadruplex Targeting Motifs on a Single Peptide Nucleic Acid Scaffold: A Hybrid (3 + 1) PNA−DNA Bimolecular Quadruplex. *Chem.—Eur. J.* **2008**, *14*, 8682−8689.
(40) Phan, A. T.; Kuryavyi, V.; Gaw, H. Y.; Patel, D. J. Small-molecule interaction with a five-guanine-tract G-quadruplex structure from the human MYC promoter. *Nat. Chem. Biol.* **2005**, *1*, 167−173.
(41) Sun, D.; Hurley, L. H. The Importance of Negative Superhelicity in Inducing the Formation of G-Quadruplex and i-Motif Structures in the c-Myc Promoter: Implications for Drug Targeting and Control of Gene Expression. *J. Med. Chem.* **2009**, *52*, 2863−2874.

https://doi.org/10.1021/jacs.3c14408
J. Am. Chem. Soc. 2024, 146, 6926−6935